

# Nuclear-reaction rates in the thermonuclear runaway phase of accreting neutron stars

M. Wiescher<sup>1,a</sup>, V. Barnard<sup>1</sup>, J.L. Fisker<sup>2,3</sup>, J. Görres<sup>1</sup>, K. Langanke<sup>3</sup>, G. Martinez-Pinedo<sup>2,3</sup>, F. Rembgès<sup>2</sup>, H. Schatz<sup>4</sup>, and F.K. Thielemann<sup>2</sup>

<sup>1</sup> Department of Physics, University of Notre Dame, Notre Dame, IN 46556-5670, USA

<sup>2</sup> Department of Physics, University of Basel, CH-4056 Basel, Switzerland

<sup>3</sup> Institute of Physics and Astronomy, University of Århus, DK-8000 Århus, Denmark

<sup>4</sup> NSCL & Department of Physics, Michigan State University, East Lansing, MI 48824, USA

Received: 21 March 2002 /

Published online: 31 October 2002 – © Società Italiana di Fisica / Springer-Verlag 2002

**Abstract.** The rp-process has been suggested as the dominant nucleosynthesis process in explosive hydrogen burning at high temperature and density conditions. The process is characterized by a sequence of fast proton capture reactions and subsequent  $\beta$ -decays. The reaction path of the rp-process runs along the drip line up to  $Z \approx 50$ . Most of the charged-particle reaction rates for the reaction path are presently based on statistical Hauser-Feshbach calculations. While these rates are supposed to be reliable within a factor of two for conditions of high density in the compound nuclei, discrepancies may occur for nuclei near closed shells or near the proton drip line where the  $Q$ -values of proton capture processes are typically very small. It has been argued that the thermonuclear runaway is less sensitive to the reaction rates because of the rapid time-scale of the event. However, since these processes may operate at the same time-scale as fast mixing and convection processes, a change in reaction rates indeed may have a significant impact. In this paper we present two examples, the break-out from the hot CNO cycles, and the thermonuclear runaway in X-ray bursts itself, where changes in reaction rates have a direct impact on time-scale, energy generation and nucleosynthesis predictions for the explosive event.

**PACS.** 21.60.Cs Shell model – 26.30.+k Nucleosynthesis in novae, supernovae and other explosive environments

## 1 Introduction

The thermonuclear runaway in accreting binary star systems is triggered by hydrogen ignition of the accreted material through the pp chains and the hot CNO cycles. Thermonuclear explosions on the surface of accreting neutron star binary components have been identified as X-ray bursts [1]. The thermonuclear explosion itself is powered by a sequence of proton capture reactions and  $\beta$ -decays on short-lived neutron-deficient nuclei [2] after break-out from the CNO cycles [3] and is characterized by the  $\approx 1$ -2 s lasting thermonuclear runaway phase at electron degenerate conditions. After degeneracy is lifted, a much longer cooling phase sets in which is typically associated with radiation-driven expansion. The endpoint of the reaction path during the entire X-ray burst is associated with reaction cycling in the Sn-Sb-Te range [4]. While the nucleosynthesis aspects of the cooling phase have been discussed in detail before [5,6], less attention

has been given to the fast ignition processes in the mass range  $A \leq 56$ . Most of the associated capture reactions are not known and for this reason are based on theoretical model predictions. Figure 1 shows the rp-process reaction path below  $Z = 34$ . The rp-process is triggered by the  $\alpha$ -capture reactions on  $^{15}\text{O}$  and  $^{18}\text{Ne}$ , which control the feeding of the rp-process range as shown in fig. 1. Both rates are not well known experimentally and are based on theoretical estimates with large uncertainties associated to them (for detailed discussion see [3]). Previous calculations of the thermonuclear runaway itself were based on global Hauser-Feshbach predictions for the reaction rates [5]. We have re-calculated the reaction rates using the nuclear-shell model in the range of  $sd$ -shell and  $fp$ -shell nuclei to improve on the nuclear-structure input and test the sensibility of the model calculations to the microscopic input [7,8]. An independent compilation of reaction rates in the  $sd$ -shell was based on mirror nuclei information to improve the calculation of resonance contributions to proton capture reactions [9]. We have performed a series of nova and X-ray burst studies using a

<sup>a</sup> e-mail: [wiescher.1@nd.edu](mailto:wiescher.1@nd.edu)

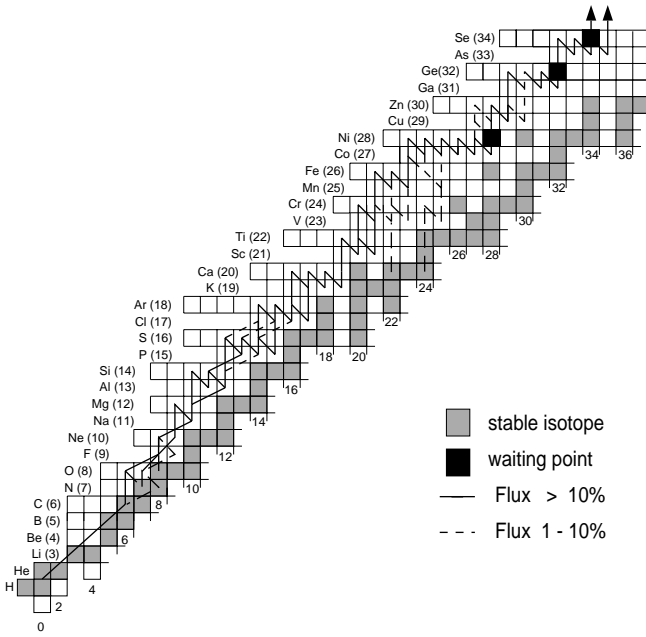


**Fig. 1.** Main reaction path of the rp-process between  $Z = 1$  and  $Z = 34$ .

self-consistent multi-zone model [10] using different sets of reaction rate predictions. It has been argued, on the basis of post-processing calculations for nova and X-ray burst nucleosynthesis, that the nuclear-reaction processes driving the thermonuclear runaway have only little impact on luminosity and nucleosynthesis development [9]. In the present paper we want to demonstrate that this is not the case. These results indicate that, due to the interplay of fast convection and reaction processes, relatively small changes in reaction rates can have a significant impact on luminosity and nucleosynthesis predictions.

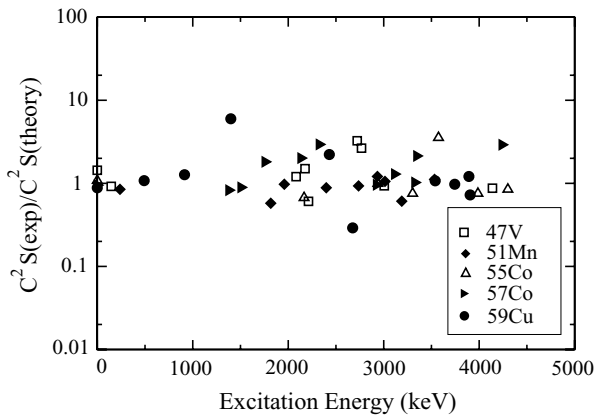


**Fig. 2.** Ratio of the experimental and calculated single-particle spectroscopic factors for states up to 4 MeV excitation energy in  $^{47}\text{V}$ ,  $^{51}\text{Mn}$ ,  $^{55}\text{Co}$ ,  $^{57}\text{Co}$ , and  $^{59}\text{Cu}$ . The average value for the ratio is  $C^2 S_{\text{exp}}/C^2 S_{\text{theory}} = 1.36 \pm 0.26$  which indicates an excellent agreement between the data and shell model predictions.

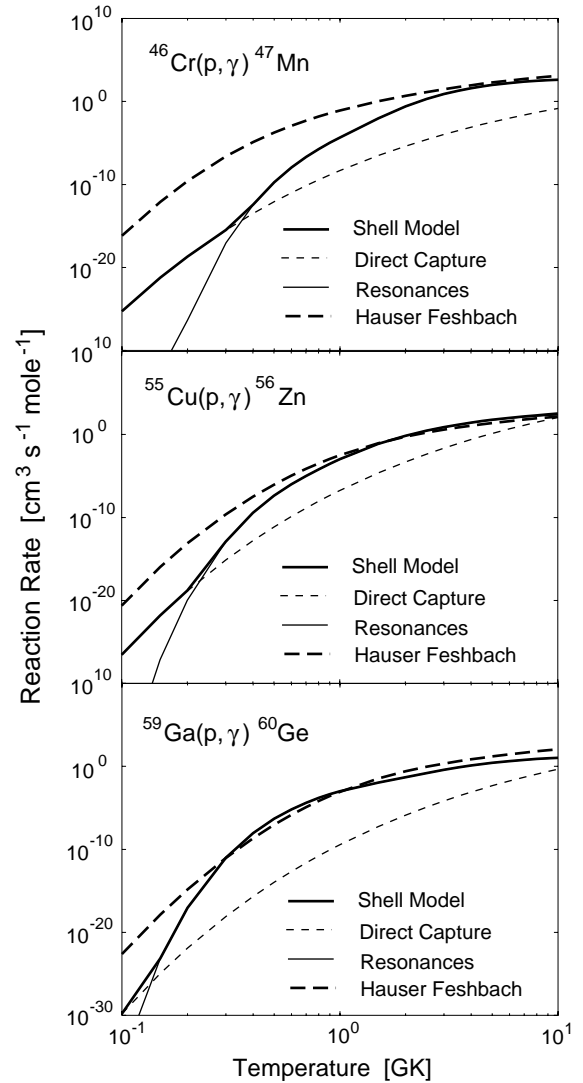


**Fig. 3.** The figure shows three examples for the comparison between Hauser-Feshbach predictions for the reaction rates of  $^{46}\text{Cr}(p, \gamma)^{47}\text{Mn}$ ,  $^{55}\text{Cu}(p, \gamma)^{56}\text{Zn}$ , and  $^{59}\text{Ga}(p, \gamma)^{60}\text{Ge}$  and the shell-model-based predictions for the direct capture and resonance contributions to the rates.

## 2 Shell-model-based reaction rates

We have used large-scale shell model diagonalization calculations to determine the level spectra, proton spectroscopic factors, and electromagnetic transition probabilities for proton-rich nuclei in the mass range  $A = 44-63$ . The calculated data were compared with experimental results available for the stable nuclei in this mass range. Figure 2 shows as an example the comparison of the calculated single-particle spectroscopic factors with available data. Based on these results on level densities, level energies and partial widths, we calculated the resonances for proton capture reactions on neutron-deficient nuclei in this mass range. We also calculated the direct capture processes on these nuclei in the framework of a Wood-Saxon potential model. Taking into account both resonant and direct contributions, we determined the

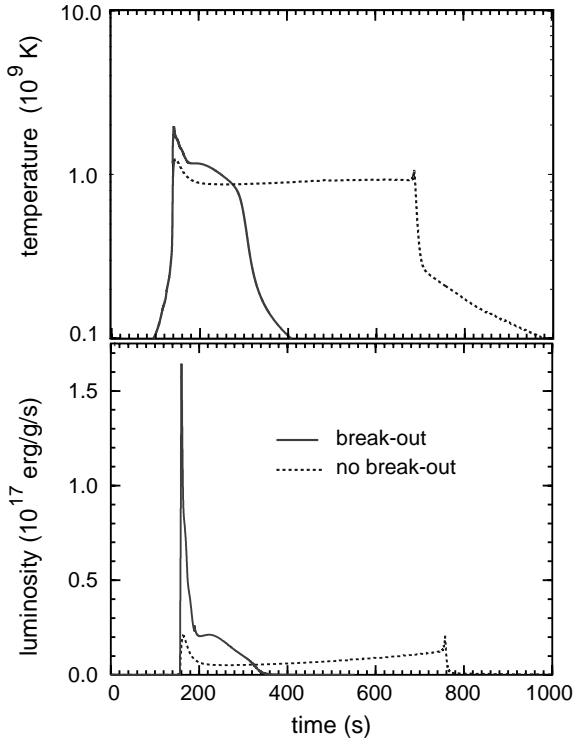


**Fig. 4.** Temperature and luminosity evolution in a one-zone X-ray burst model. The solid curve indicates the rapid temperature and luminosity increase associated with the rp-process-driven thermonuclear runaway, the dashed curve reflects a steady hot CNO burning fueled by  $^{12}\text{C}$  production through the triple- $\alpha$ -process.

proton capture reaction rates for these nuclei under hot hydrogen burning conditions for temperatures between  $10^8$  K and  $10^{10}$  K [8]. These shell-model-based (SM) reaction rates were compared with recently published Hauser-Feshbach (HF) rate predictions for proton capture rates in this mass range [5,11]. While in most cases good agreement has been obtained, for several reactions along the reaction path near the proton drip line significant discrepancies between the HF and the SM predictions were observed. Figure 3 shows three examples where the HF rate is predicted to be significantly larger than the SM rate over a wide temperature range.

### 3 Impact of reaction rates on type-I X-ray burst simulation

Type-I X-ray bursts have been associated with the unstable burning on H/He accreting neutron stars resulting in regular outbursts of periodic time-scales from a few minutes to days [1]. The onset of the X-ray burst is thermonuclear runaway which is driven by the energy release in the rp-process. The rp-process itself is triggered by the two break-out reactions,  $^{15}\text{O}(\alpha, \gamma)^{19}\text{Ne}$  and  $^{18}\text{Ne}(\alpha, p)^{21}\text{Na}$ . The associated reaction rates control the onset, the reaction flow, and subsequently the luminosity of the burst. Presently, the rates are only based on estimated resonance

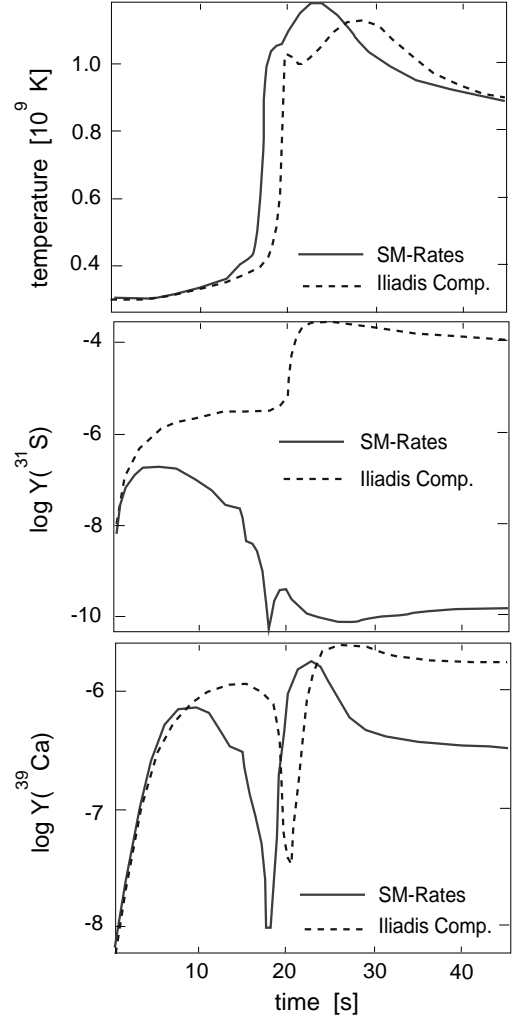


**Fig. 5.** Comparison of the temperature profile and the  $^{31}\text{S}$ ,  $^{39}\text{Ca}$  abundance development during the X-ray burst for different sets of reaction rates for proton capture on  $^{27}\text{Si}$ ,  $^{31}\text{S}$ ,  $^{35}\text{Ar}$ , and  $^{39}\text{Ca}$ .

strengths which could be largely over-estimated as discussed in previous work [3]. Figure 4 shows a calculation for the temperature and luminosity development in a one-zone X-ray burst model [6] comparing the presently suggested rate with an experimental lower limit which does not include the estimated lower-energy resonance contributions. In the second case the break-out is basically inhibited and the hydrogen fuel is burned over a much longer time-scale in a triple- $\alpha$ -process-driven hot CNO cycle.

While these break-out reactions on CNO isotopes trigger the X-ray burst capture, reactions on higher mass isotopes can cause significant pre-heating of the material and a considerable change in abundance distribution prior the runaway. This in conjunction with rapid mixing of material in and out of burning regions can cause a significant change in the morphology of the burst. To simulate the burst dynamics and the associated luminosities, we have used an implicit one-dimensional code, which solves the hydrodynamical equations suitable for a neutron star [10].

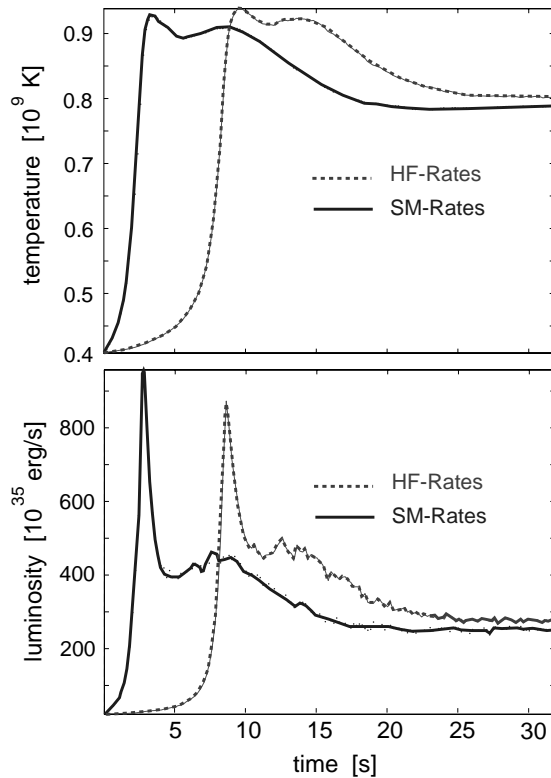


**Fig. 6.** Comparison of the temperature and luminosity evolution during the thermonuclear runaway of an X-ray burst for different sets of proton capture rates in the  $Z = 22-36$  range.

The accretion layer is divided into 150 zones covering the range between  $\rho = 10^4-10^7$  g/cm<sup>3</sup> with a high grid point resolution in the hot burning zone ( $\rho \sim 10^6$  g/cm<sup>3</sup>). The hydrodynamics is coupled explicitly to a full network of 208 selected isotopes between <sup>1</sup>H and <sup>94</sup>Pd [12]. We have compared the influence of the capture reaction rates on *sd*-shell nuclei [7, 9] for the early phase of the thermonuclear runaway after the break-out occurred. In contrast to earlier statements [9], the present calculation with a multi-zone mass model shows significant rate dependencies both in expansion velocity and radius, temperature and luminosity, as well as in abundance development [10]. Figure 5 shows as an example the temperature evolution and the development of the <sup>31</sup>S and <sup>39</sup>Ca abundances which represent major impedances for the rp-process reaction flow at lower temperatures. These discrepancies are mainly due to the difference in rp-process burning of the initial Si to Ca abundances prior to break-out. The higher SM rates cause pre-heating of the material in the burning zones and subsequently a more rapid evolution of the abundances.

In a second study we have investigated the significance of the SM rates in the *pf*-shell [8] by comparing them to the HF rates discussed in the previous section. The use of the SM rates triggers the burst at an earlier point in time. This can be observed both in the temperature development during the burst as well as in the associated luminosity evolution shown in fig. 6. The SM rates above  $A = 50$  are generally faster than the HF rates at the here consid-

ered temperature and density conditions, but they cause only small and insignificant changes in the burst evolution. The reactions mainly responsible for the altered burst behavior are capture processes on isotopes with  $A \leq 56$  like <sup>45</sup>V(p,  $\gamma$ ), <sup>46</sup>V(p,  $\gamma$ ), <sup>47</sup>V(p,  $\gamma$ ), and <sup>49</sup>Mn(p,  $\gamma$ ). Compared to the corresponding HF rates in the temperature window of the burst, the SM rates on V isotopes are about a factor two stronger, which, due to the exponential temperature dependence of the rates combined with the feedback from the enhanced energy generation, leads to the early burst. On the other hand, the <sup>49</sup>Mn(p,  $\gamma$ ) SM rate is considerably weaker compared to the HF prediction. It therefore resembles a major impedance for the pre-burst reaction flow. However, this re-routes the reaction path to a faster string of reaction links above  $A = 50$  which subsequently feeds the burst.

## 4 Conclusion

It has been shown that single reaction rates can have significant direct and indirect impact on the evolution of the thermonuclear runaway in an X-ray burst. This is caused by pre-burst heating and nucleosynthesis effects through fast reactions in different layers, but also by hydrodynamic feedback, mixing material in and out of burning zones at time-scales comparable to the nuclear-reaction time-scales. While we have only compared X-ray models for different sets of theoretical reaction rates, these results indicate that a more precise determination of specific reaction rates is important if precise knowledge of the burst evolution is desired.

## References

1. R.E. Taam, S.E. Woosley, D.Q. Lamb, *Astrophys. J.* **459**, 271 (1996).
2. L. van Wormer, J. Görres, C. Iliadis, M. Wiescher, F.-K. Thielemann, *Astrophys. J.* **432**, 326 (1994).
3. M. Wiescher, J. Görres, H. Schatz, *J. Phys. G: Nucl. Phys.* **25**, R133 (1999).
4. H. Schatz, A. Aprahamian, V. Barnard, L. Bildsten, A. Cummin, M. Ouellette, T. Rauscher, F.-K. Thielemann, M. Wiescher, *Phys. Rev. Lett.* **86**, 3471 (2001).
5. H. Schatz, A. Aprahamian, J. Görres, M. Wiescher, T. Rauscher, J.F. Rembges, F.-K. Thielemann, B. Pfeiffer, P. Möller, K.-L. Kratz, H. Herndl, B.A. Brown, H. Rebel, *Phys. Rep.* **294**, 168 (1998).
6. M. Wiescher, H. Schatz, *Prog. Theor. Phys.* **140**, 11 (2000).
7. H. Herndl, J. Görres, M. Wiescher, B.A. Brown, L. van Wormer, *Phys. Rev. C* **52**, 1078 (1995).
8. J.L. Fisker, V. Barnard, J. Görres, K. Langanke, G. Martinez-Pinedo, M. Wiescher, *At. Nucl. Data Tables*, <http://www.idealibrary.com/links/doi/10.1006/adnd.2001.0867/pdf>.
9. C. Iliadis, P.M. Endt, N. Prantzos, W.J. Thompson, *Astrophys. J.* **524**, 434 (1999).

10. F.-K. Thielemann, F. Brachwitz, C. Freiburghaus, E. Kolbe, G. Martinez-Pinedo, T. Rauscher, F. Rembges, W.R. Hix, M. Liebendörfer, A. Mezzacappa, K.-L. Kratz, B. Pfeiffer, K. Langanke, K. Nomoto, S. Rosswog, H. Schatz, M. Wiescher, *Prog. Part. Nucl. Phys.* **46**, 5 (2001).
11. T. Rauscher, F.-K. Thielemann, *At. Data Nucl. Data Tables* **75**, 1 (2000).
12. F. Rembges, C. Freiburghaus, T. Rauscher, F.-K. Thielemann, H. Schatz, M. Wiescher, *Astrophys. J.* **484**, 412 (1997).